

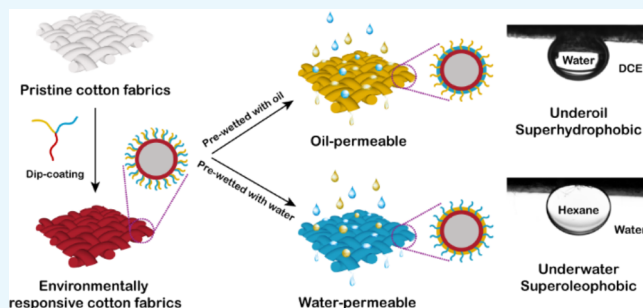
# On-Demand Oil–Water Separation by Environmentally Responsive Cotton Fabrics

Meina Xiao, Yinghui Huang, Anli Xu, Tongtong Zhang, Chengdong Zhan, and Liangzhi Hong\*<sup>✉</sup>

Department of Polymer Materials Science and Engineering, South China University of Technology, Guangzhou 510641, China

**S** Supporting Information

**ABSTRACT:** Environmentally responsive cotton fabrics were fabricated by dip-coating ABC miktoarm star terpolymers, which contain reactive poly(3-triisopropoxypropyl methacrylate) blocks, hydrophobic poly(dimethylsiloxane) (PDMS) blocks, and hydrophilic poly(*N,N*-dimethylaminoethyl methacrylate) (PDMAEMA) blocks. The functionalized cotton fabrics with perfectly alternating PDMS and PDMAEMA blocks show underoil superhydrophobicity and underwater superoleophobicity. The wettability and permeability of the functionalized fabrics can be readily adjusted by the contacting medium. More interestingly, surface reconstruction causes a reduction in the breakthrough pressure of the nonwetting phase. The adaptive permeability endows the functionalized cotton fabrics with the capability to separate heavy oil–water–light oil ternary mixtures.



## INTRODUCTION

Efficient separation of oil–water mixtures is a worldwide environmental challenge due to the frequent oil spills and the increasing oily wastewater generated from chemical industry and metal finishing.<sup>1,2</sup> In membrane filtration processes, surface wettability is crucial to efficient oil–water separation.<sup>3–5</sup> Two types of special wetting membranes have been intensively investigated in the past two decades, namely superhydrophobic/superoleophilic and superhydrophilic/underwater superoleophobic membranes.<sup>6–12</sup> However, choosing the appropriate membrane is critical to separating various oil–water mixtures in order to avoid the membrane being blocked by the nonpermeable phase.<sup>13,14</sup> For example, the superhydrophobic/oleophilic surfaces is not suitable for separating mixtures of water and light oil based on gravity separation. When water is first contacted with the superhydrophobic membrane, the separation process is hindered, and a specially designed separation apparatus is needed.

Smart surfaces with switchable wettability have been reported for oil–water separation in response to external stimuli such as pH,<sup>15–21</sup> temperature,<sup>22–25</sup> light,<sup>26</sup> and electric field.<sup>27,28</sup> Block copolymers comprising the pH-responsive block were coated onto different substrates to impart switchable wettability to the prepared membranes.<sup>15–17</sup> For the membrane modified with polydimethylsiloxane-*b*-poly(2-vinylpyridine) (PDMS-*b*-P2VP), the membrane was oleophilic and the oil penetrated the mesh when pretreated with basic aqueous solution. Conversely, when the fabric was prewetted with acidic aqueous solution, water was found to penetrate the fabric.<sup>17</sup> The protonation and deprotonation of the pyridine groups altered the polarity of the surface and thus changed the

surface wettability. In addition, switchable wettability triggered by other stimuli, such as ammonia,<sup>21</sup> carbon dioxide,<sup>29</sup> stearic acid with solvent<sup>30</sup> and temperature,<sup>22–24</sup> as well as thermo- and pH dual-responsive<sup>25</sup> have been reported. However, the abovementioned methods require ex situ treatments to trigger the change of surface wettability, which is inappropriate for successive oil–water separation. Therefore, in situ wettability switch is highly desirable to effectively separate complex oil–water mixtures.<sup>31</sup> Tuteja and coworkers prepared a novel hygro-responsive membrane using a mixture of hydrophobic fluorodecyl POSS and hydrophilic poly(ethylene glycol) diacrylate.<sup>32</sup> The membrane surface is superhydrophilic and superoleophobic in air or under water due to surface reconfiguration caused by the contacting medium. Liu's group have developed an innovative janus membrane for separating oil from oil-in-water (O/W) emulsions where the polyamine-bearing side causes demulsification, and the PDMS-bearing side selectively allows oil to pass.<sup>33</sup> They further improved the coating procedure with designed block copolymers and demonstrated the use of these janus membranes for rapid separation of oil from various surfactant-stabilized O/W emulsions.<sup>34,35</sup>

Most studies used simple oil–water mixtures to demonstrate the separation efficiency, which is quite different from actual oil spills and industrial wastewater.<sup>8</sup> The challenge of continuously separating heavy oil–water–light oil ternary mixtures still exists, which is common in actual oil spill cases.<sup>19</sup> Noting that

**Received:** April 30, 2019

**Accepted:** July 8, 2019

**Published:** July 18, 2019

heavy oil refers to oil with a density greater than water, while light oil refers to oil with a density less than water. Continuous in situ separation of heavy oil–water–light oil ternary mixtures provides a new strategy for handling oil spills. Ju and coworkers fabricated a pH-responsive surface for the controllable separation of oil–water ternary mixtures.<sup>19</sup> The initial superhydrophobic membrane allowed the bottom oil layer to penetrate, whereas the water was retained. The permeation of water through the membrane was then triggered by adding an aqueous alkaline solution to increase the pH value of the water phase. Eventually, the light oil was blocked by the superhydrophilic surface.<sup>19</sup> Cao and coworkers designed a dually prewetted cotton fabric for separating the oil–water ternary mixtures.<sup>36</sup> Fabrics coated with corn straw powder and polyurethane can be wetted by both oil and water. Oil and water were selectively permeated through the oil-prewetted area and water-prewetted area, respectively.<sup>36</sup> Very recently, a dually prewetted carbon black-coated PVDF microfiltration membrane has been reported for the continuous separation of multiphase emulsion mixtures.<sup>37</sup>

Here, we report the fabrication of an environmentally responsive cotton fabrics and discuss the use of the functionalized fabrics to separate complex oil–water mixtures. The environmentally responsive membrane was prepared by grafting ABC miktoarm star terpolymers onto cotton fabrics as shown in Figure 1. The designed ABC miktoarm star

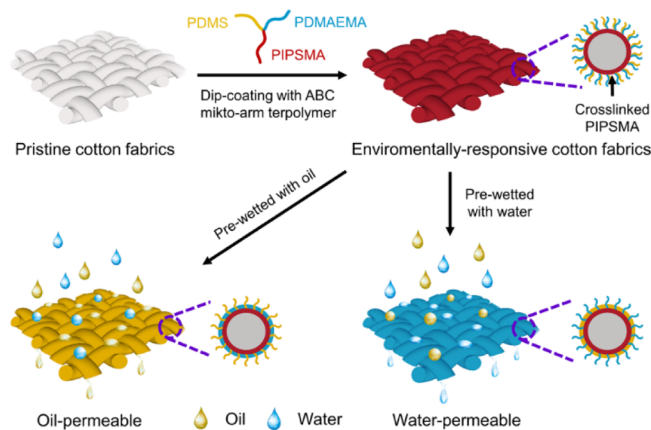


**Figure 1.** Schematic of an environmentally responsive cotton fabrics fabricated by coating a  $\mu$ -PDMS-*b*-PDMAEMA-*b*-PIPSMA ABC miktoarm terpolymer and its permeability after contact with oil or water.

terpolymers are  $\mu$ -poly(dimethylsiloxane)-*b*-poly(*N,N*-dimethylaminoethyl methacrylate)-*b*-poly(3-triisopropoxypropyl methacrylate) ( $\mu$ -PDMS-*b*-PDMAEMA-*b*-PIPSMA). The PIP SMA block can form a cross-linked layer on cotton fabric via sol–gel reaction between the triisopropoxypropyl groups and surface hydroxyl groups of cotton. PDMS and PDMAEMA blocks can then be mounted on cotton fabrics and arranged in a strictly alternating pattern. The glass-transition temperatures of PDMS and PDMAEMA block are around  $-124$  and  $19$  °C, respectively.<sup>38,39</sup> A lower glass-transition temperature facilitates surface reconfiguration induced by the contact medium. In the oil medium, the hydrophobic PDMS is distributed outside the cotton fabrics, and the hydrophilic PDMAEMA is segregated into the interior of the shell. These surface structures will then exhibit hydrophobicity and selectively pass oil through the membrane. In contrast, in the

aqueous medium, the outer shell of cotton fabrics consists of stretched PDMAEMA chains and collapsed PDMS chains, and these structures will exhibit hydrophilicity and preferably pass water through the membrane. We have recently reported environmentally responsive hairy particles with regulatable surface wettability for the preparation of tunable Pickering emulsions.<sup>40</sup> Liu and coworkers also reported organohydrogels with reconfigurable heteronetwork structures and adaptive surface wettability.<sup>41</sup> We have demonstrated that the functionalized cotton fabrics with adaptive permeability can be used to separate complex oil–water mixtures.

## RESULTS AND DISCUSSION

A family of amphiphilic ABC miktoarm star terpolymers consisting of PDMS, PDMAEMA, and PIP SMA were synthesized according to our previous reported procedure, as shown in Figure 2.<sup>40</sup> Under the click reaction conditions, the

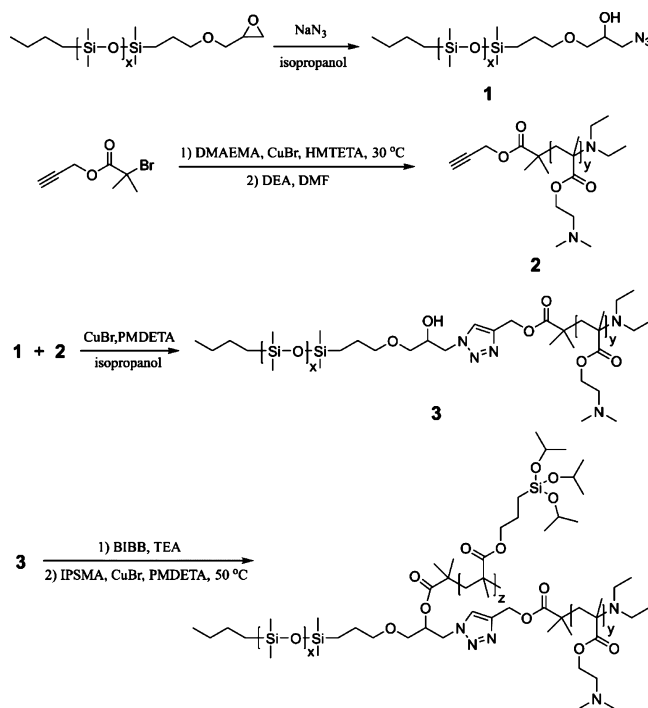


**Figure 2.** Schematic synthesis of  $\mu$ -PDMS<sub>*x*</sub>-*b*-PDMAEMA<sub>*y*</sub>-*b*-PIPSMA<sub>*z*</sub> miktoarm star terpolymers.

halide groups of the PDMAEMA block will generate radicals, which will result in undesirable branching and cross-linking.<sup>42</sup> Therefore, excessive diethylamine was added to dehalogenate the PDMAEMA block before click reactions.<sup>43</sup> The ABC miktoarm star terpolymers are labeled as  $\mu$ -PDMS<sub>*x*</sub>-*b*-PDMAEMA<sub>*y*</sub>-*b*-PIPSMA<sub>*z*</sub> (P1, P2, and P3), wherein the subscripts indicate the degree of polymerization of the respective blocks. Figure 3 shows <sup>1</sup>H NMR spectra of  $\mu$ -PDMS<sub>*x*</sub>-*b*-PDMAEMA<sub>*y*</sub>-*b*-PIPSMA<sub>*z*</sub> (P2) and the peak assignments. The characteristic peak of PDMS is observed at 0.07 ppm (a) for the protons of the methyl groups ( $-\text{Si}(\text{CH}_3)_2-$ ). The peaks at 2.56 (c) and 4.06 ppm (d) are protons of the methylene group for PDMAEMA. The peaks at 3.87 (h) and 0.55 (g) are attributed to the methylene protons adjacent to the ester group and silicon of PIP SMA, respectively. Table 1 lists the characteristics of  $\mu$ -PDMS<sub>*x*</sub>-*b*-PDMAEMA<sub>*y*</sub>-*b*-PIPSMA<sub>*z*</sub> miktoarm star terpolymers. For the three ABC miktoarm

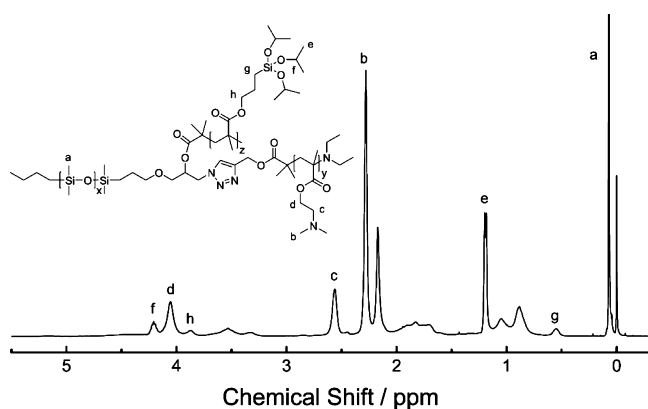


**Figure 3.**  $^1\text{H}$  NMR spectra of  $\mu\text{-PDMS}_x\text{-}b\text{-PDMAEMA}_y\text{-}b\text{-PIPSMA}_z$  (P2) in  $\text{CDCl}_3$ .

**Table 1. Characteristics of  $\mu\text{-PDMS}_x\text{-}b\text{-PDMAEMA}_y\text{-}b\text{-PIPSMA}_z$  ABC Miktoarm Star Terpolymers**

	$x$	$y$	$z$	$M_n$ ( $\times 10^4$ g/mol) <sup>a</sup>	PDI <sup>b</sup>
P1	64	42	22	1.92	1.30
P2	64	121	24	3.23	1.29
P3	64	148	25	3.68	1.26

<sup>a</sup>Determined by  $^1\text{H}$  NMR. <sup>b</sup>Determined by SEC.

star terpolymers P1, P2, and P3, the PDMS block length is the same ( $x = 64$ ), and the PDMAEMA block lengths are 42, 121, and 148, respectively. The surface composition and surface wettability of cotton fabrics are adjusted by the block length of PDMAEMA.

The interthread pore size of the cotton fabric used is  $60\ \mu\text{m}$  (Figure S13). To coat the fabric swatches, a  $3 \times 3\ \text{cm}^2$  sample was immersed in corresponding polymer solution (30 mg/mL) for 30 min. The sample was withdrawn from the solution and then heated at  $180\ ^\circ\text{C}$  for 4 h under vacuum. Subsequently, the fabrics were extracted in tetrahydrofuran (THF) for 8 h using a Soxhlet extractor to remove unreacted block copolymers. After extraction, the fabric samples were dried under vacuum for 24 h. The functionalized cotton fabrics are denoted as P1@CF, P2@CF, and P3@CF. The mass fraction of the grafted block copolymer in the functionalized cotton fabrics was determined by gravimetric analysis to be 7–11% (Figure S14, Table S2).

As shown in the scanning electron microscopy (SEM) image (Figure 4a), the pristine cotton fabric has a smooth surface. After coating with ABC miktoarm terpolymers (P3), the surface roughness increases as shown in Figure 4b. The combination of the SEM image and energy-dispersive X-ray spectroscopy (EDS) analysis is a powerful technique for determining the surface composition and composition distribution.<sup>34</sup> Figure 4c,d shows the SEM–EDS images of P3@CF. The yellow dots representing the Si element (Figure 4c), which is belonged to the PDMS block, are uniformly distributed on the surface of the fabric. Similarly, the blue dots in Figure 4d representing the N element, which is belonged to the PDMAEMA block, are also uniformly distributed on the fabric surface. The merged yellow and blue dots unambiguously support the successful fabrication of targeted cotton fabric with alternating hydrophobic PDMS and hydrophilic PDMAEMA. These results are consistent with X-ray photoelectron spectroscopy (XPS) of functionalized cotton fabrics (Figure S15). Noting that the mixed polymer brushes with alternative distribution differ from recently reported V-shape structures.<sup>17,34,35,44</sup>

In air, the hydrophobic PDMS block is distributed outside the fabric surface, so the surface initially exhibits hydrophobicity and lipophilicity, as shown in Figure 4e. Hexane soaks into functionalized cotton fabrics rapidly, and the water contact angle (CA) is  $120^\circ$ . However, the water CA of the functionalized fabrics (Figure 4f) gradually decreases over time as compared to the rapid wetting of the pristine cotton fabrics. The water droplet causes the hydrophilic PDMAEMA to be exposed to the exterior, and the hydrophobic PDMS to collapse into the interior to minimize the surface energy. Because PDMAEMA has a  $\text{p}K_a$  of 8.0,<sup>45</sup> the pendant dimethyl groups can be protonated in deionised (DI) water, which has been confirmed by in situ attenuated total reflection–Fourier transform infrared (ATR–FTIR) spectroscopy analysis (Figure 5a). In hexane, the characteristic  $1720\ \text{cm}^{-1}$  band was attributed to the stretching of  $\text{C}=\text{O}$  groups of swelled PDMAEMA. In DI water, the protonated dimethyl amino group is capable of forming ring conformation with the carbonyl group through the hydrogen bond, as shown in Figure 5b. Because of hydrogen bonding, the characteristic band of the carbonyl group shifts to  $1640\ \text{cm}^{-1}$ .<sup>46</sup> The evolution of the water CA in air clearly indicates the process of

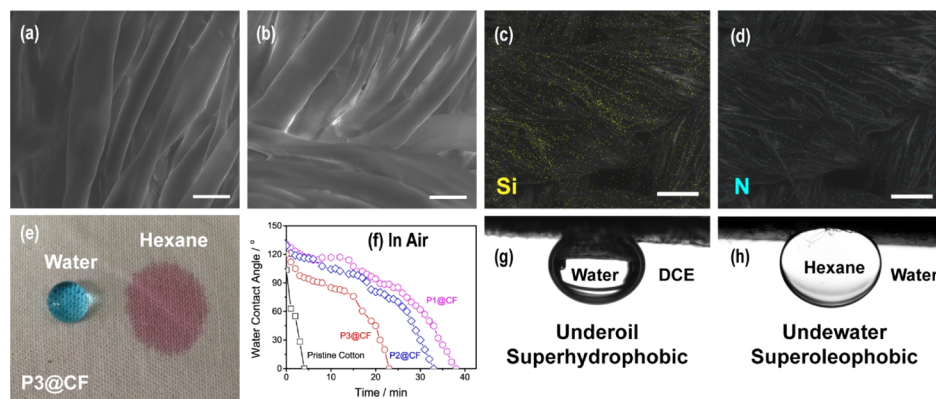


**Figure 4.** SEM images of (a) pristine cotton fabric and (b) cotton fabrics coated with ABC miktoarm terpolymer P3 (P3@CF). (c,d) EDS elemental mapping of silicon and nitrogen corresponding to P3@CF. (e) Droplets of water and hexane on P3@CF. (f) Evolution of water CAs in air of the functionalized cotton fabrics over time. (g) Underoil water CA, and the oil is 1,2-dichloroethane (DCE). (h) Underwater oil CA. The oil is hexane. The scale bars in (a,b) are  $20\ \mu\text{m}$ , and the scale bars in (c,d) are  $50\ \mu\text{m}$ .

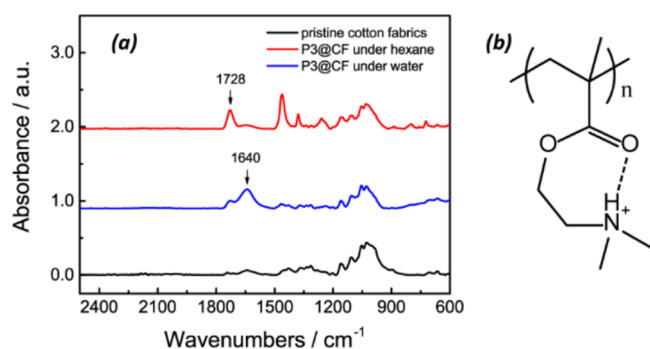


**Figure 5.** (a) ATR–FTIR of pristine cotton and P3@CF in water and hexane. (b) Protonated PDMAEMA ring conformation formed by intramolecular hydrogen bonding.

surface reconfiguration and wettability switching induced by water droplets.<sup>32,35</sup> As the volume fraction of PDMAEMA increases from 49.3% (P1@CF) to 77.4% (P3@CF), the time to complete wetting was reduced from 38 to 23 min. For longer PDMAEMA chains, the textured surface can be reconstructed more easily. Because of surface reconstruction, the functionalized cotton fabrics can be wetted by both oil and water. As shown in Figure 4g,h, the functionalized fabrics display unusual underoil superhydrophobic and underwater superoleophobic. The underoil water CA is 151°, and the underwater oil CA is 152°. Previously, these dual superlyophobic states were considered to be energetically unfavorable for a given surface.<sup>47</sup> Tian and coworkers created such a dual superlyophobic surface through the combination of delicate re-entrant topography and finely matched surface chemistry.<sup>47</sup> However, in our approach, the dual superlyophobic surface can be constructed by simple dip-coating of ABC miktoarm star terpolymers. The underwater and underoil wetting properties for functionalized cotton fabrics coated with P1 and P2 (P1@CF, P2@CF) are shown in Figure S16. As the PDMAEMA block length increases, the underoil CA decreases slightly, while the underwater oil CA increases.

The breakthrough pressure ( $P_{bt}$ ) is an important parameter for gravity-driven oil–water separation, which is the critical pressure required to force a nonwetting phase to penetrate a membrane that is infused with a wetting phase.<sup>32,48</sup> As shown in the inset photographs in Figure 6, hydrostatic testing has been utilized to determine the breakthrough height ( $h_{bt}$ ) of hexane and water. For functionalized cotton fabrics, the  $h_{bt}$  of hexane is around 21 cm, and the  $h_{bt}$  of water is around 10 cm. These  $h_{bt}$  values are higher than the reported  $h_{bt}$  of hygro-

responsive membranes obtained by dip-coating fluorodecyl POSS and poly(ethylene glycol) diacrylate, which is around 1.3 cm for water and oil.<sup>32</sup> The higher value of  $h_{bt}$  facilitates the oil–water separation process by increasing the operating height. Accordingly, the breakthrough pressure can be calculated from the breakthrough height by  $P_{bt} = \rho gh_{bt}$ , here  $\rho$  is the liquid density and  $g$  is the gravitational acceleration. For the functionalized cotton fabrics, the breakthrough pressure of hexane and water can be well tuned by adjusting the relative block length of PDMAEMA and PDMS on the membrane surface as shown in Figure 6a,b. The breakthrough pressure of hexane on the functionalized cotton fabrics pretwetted by water increases as the block length of PDMAEMA increases. This trend is reasonable because the longer PDMAEMA block pretwetted with water will provide a stronger barrier to hexane and consequently inhibit hexane penetration. Conversely, as shown in Figure 6b, the breakthrough pressure of water on the functionalized cotton fabrics pretwetted with hexane decreases as the block length of PDMAEMA increases. A longer PDMAEMA block length is easier to reach the coating surface and promote the water penetration, thus reducing water breakthrough pressure.

The functionalized cotton fabrics with switchable wettability can be applied to separate both light oil–water mixtures and heavy oil–water mixtures. As shown in Figure 7a and Movie S1, using an oil-pretwetted cotton fabrics (P1@CF), 1,2-dichloroethane (DCE) readily penetrated the functionalized textile, and water was retained above the membrane. However, when the textile was pretwetted by water, water passed through the membrane, and hexane was retained (Figure 7b and Movie S2). The adaptive permeability of the textiles to oil or water makes them useful for different oil–water separation processes. This multifunctional material has been rarely reported in terms of selective oil–water separation.<sup>32</sup> The efficiency of separation is determined by comparing the weight of water or oil before and after separation. For dichloroethane–water mixtures, the separation efficiency for P1@CF is  $93.3 \pm 4.4\%$ . For water–hexane mixtures, the separation efficiency for P1@CF is  $97.3 \pm 2.5\%$ . They remain highly efficient after 20 cycles, as shown in Figures S17 and S18.

More importantly, we have found that the retained nonwetting phase below the breakthrough height can also pass through the functionalized fabrics after a certain block time. In other words, for environmentally responsive cotton fabrics, the breakthrough height or breakthrough pressure of the nonwetting phase gradually decreases. For the water phase with 7.6 cm height (below the breakthrough height) on P1@

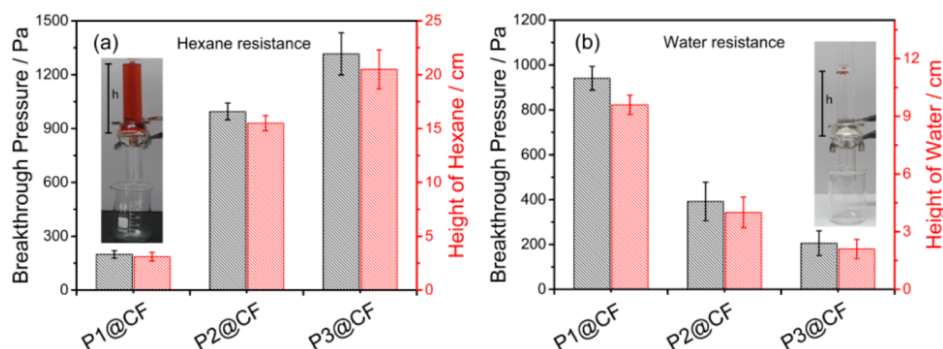
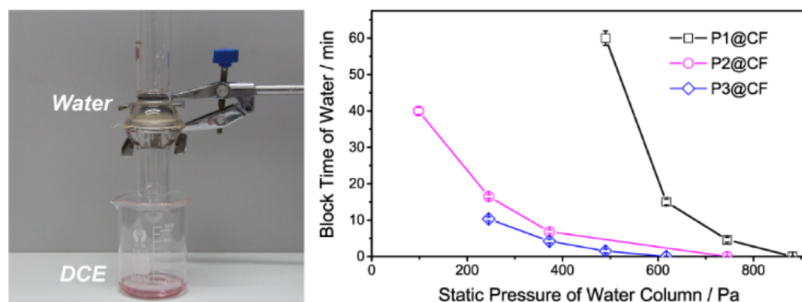


**Figure 6.** (a) Breakthrough pressure of hexane on the functionalized cotton fabrics pretwetted by water. (b) Breakthrough pressure of water on the functionalized cotton fabrics pretwetted by hexane.

## (a) Separation of DCE/water mixtures



## (b) Separation of water/hexane mixtures

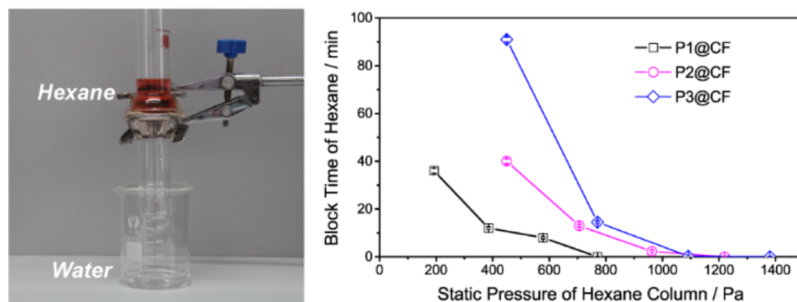


**Figure 7.** Photographs of the oil–water separation experiments, includes (a) separation of DCE–water, (b) separation of water–hexane. The figures in (a,b) are block time of the liquid phase related to the static pressure of the respective liquid column.

CF, the block time is around 4.6 min. After this, water completely pass through the fabrics. As shown in Figure 7a,b, the block time for water and hexane decreases drastically as the static pressure of liquid column increases.

For fabrics, the breakthrough pressure ( $P_{bt}$ ) is given as

$$P_{bt} = \frac{2R\gamma_{12}}{D^2} \frac{1 - \cos(\theta')}{1 + 2\left(\frac{R}{D}\right) \sin(\theta')}$$

here  $R$  is the cylinder radius,  $D$  is the half of the intercylinder spacing,  $\gamma_{12}$  is the interfacial tension between the wetting and nonwetting phases, and  $\theta'$  is the CA of the nonwetting liquid droplet on the fabric surface in the wetting phase.<sup>32,49</sup> After the wetting phase passes through the membrane, the nonwetting phase will begin to contact the membrane surface and cause the surface reconstruction. Therefore, the CA will decrease as the lipophilic polymer block accumulates in the surface. From the above equation, the breakthrough pressure decreases as the CA decreases (Figure S19). Then, when the continuously decreasing CA approaches a critical value, the nonwetting phase penetrates the membrane. Both the wetting and nonwetting phase can be infiltrated through the environmentally responsive cotton fabrics. The block time of the nonwetting phase to penetrate the membrane is closely related to the surface composition of cotton fabrics. For example, the block time of water to pass through cotton fabric pretreated with DCE decreases as the PDMAEMA block length increases.

Inspired by the  $P_{bt}$  changes caused by surface reconstruction, we hypothesize that the environmentally responsive cotton fabrics can be used for the separation of heavy oil–water–light oil ternary mixtures as shown in Figure 8a. The surface wettability of such membrane depends on the contact medium, and when the wetting phase is completely infiltrated and the nonwetting phase begins to contact the surface, the change in the medium will trigger in situ wettability switching. When the

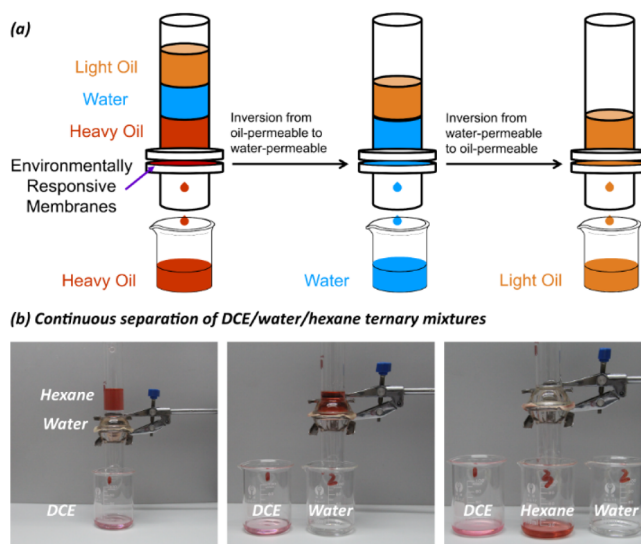


**Figure 8.** (a) Schematic diagram of the separation of heavy oil–water–light oil ternary mixtures using an environmentally responsive membrane. (b) Photographs of continuous separation of DCE–water–hexane ternary mixtures.

heavy oil is completely infiltrated and water begins to contact the membrane, the permeability of the membrane changes from oil-permeable to water-permeable through surface reconfiguration induced by the aqueous phase. Similarly, when the water is completely infiltrated and the light oil begins to contact the membrane, an inversion from water-permeable to oil-permeable occurs. Therefore, the environmentally responsive membranes are oil-permeable when exposed to heavy oils and light oils, and they are water-permeable when exposed to the aqueous phase without resorting to ex situ stimulus. As shown in Figure 8b and Movie S3, DCE, water,

and hexane pass through the membrane sequentially. DCE immediately penetrates the P1@CF membranes, and water and hexane pass through the membrane with the block time of 17 and 1 min, respectively. For dichloroethane–water–hexane ternary mixtures, the separation efficiency for P1@CF in the first stage is  $93.7 \pm 1.3\%$ , and the separation efficiency in the second stage is  $99.4 \pm 0.2\%$ . They remain highly efficient after 10 cycles, as shown in Figure 9.

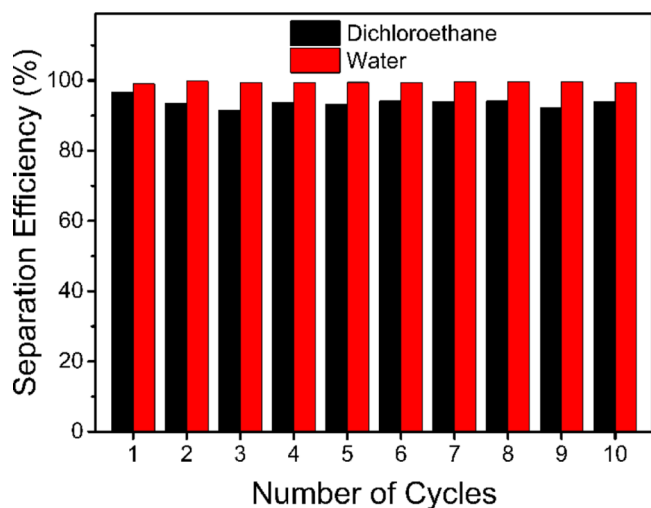


**Figure 9.** Oil–water separation efficiency vs recycle numbers for the separation of dichloroethane–water–hexane ternary mixtures. The membrane used is P1@CF. The efficiency of separation is determined by comparing the weight of water or oil before and after separation.

## CONCLUSIONS

In summary, environmentally responsive cotton fabrics were fabricated by a simple sol–gel reaction between the triisopropoxyethyl groups of the ABC miktoarm terpolymer and the surface hydroxyl group of cotton. The wettability and permeability of the functionalized fabrics can be regulated by the contacting medium. The functionalized cotton fabrics shows underoil superhydrophobicity and underwater superoleophobicity. In addition, the breakthrough pressure of these fabrics can be finely adjusted by changing the volume fraction of hydrophilic and hydrophobic blocks. More importantly, the breakthrough pressure decreases as the contact time with the nonwetting phase increases. We have demonstrated that this environmentally responsive fabric can be used to separate heavy oil–water–light oil ternary mixtures. Combined with the demulsification capability by coating this polymer onto membranes with smaller pores, the environmentally responsive membranes may find practical applications in the separation of complex oil–water mixtures.<sup>50</sup>

## EXPERIMENTAL SECTION

**Materials.** PDMS monoglycidyl ether terminated (PDMS epoxy terminated,  $M_n = 5000$  g/mol, Aldrich), 1,4,7,7-pentamethyl diethylenetriamine (PMDETA, 99%, Aldrich), hexamethyltriethylenetetramine (HMTETA, 99%, Aldrich), propargyl alcohol (99%, Aldrich), sodium azide (99%, Energy Chemical Reagent Co.), isopropanol (99%, Energy Chemical Reagent Co.), 2-bromo-2-methylpropionyl bromide (98%, Energy Chemical Reagent Co.), and acetic acid (99%, Energy Chemical Reagent Co.) were used as received. *N,N*-

Dimethylaminoethyl methacrylate (DMAEMA, 98%, Aladdin) was dried over  $\text{CaH}_2$  for 24 h at room temperature followed by distillation under vacuum before use. 3-(Triisopropoxyethyl)propyl methacrylate (IP SMA) was synthesized according to the literature method.<sup>51</sup> CuBr was washed sequentially with acetic acid and anhydrous ethanol and then dried under vacuum at 60 °C. Triethylamine (TEA) was purified by refluxing with *p*-toluenesulfonyl chloride and distilled under a  $\text{N}_2$  atmosphere before use. Cotton fabric was purchased from a local store. The fabric was washed with a 5.0 wt % detergent aqueous solution thrice before rinsing with distilled water ten times, acetone thrice, and drying under vacuum for 24 h.

**Synthesis of ABC Miktoarm Star Terpolymers:  $\mu$ -Poly(dimethylsiloxane)-*b*-poly(*N,N*-dimethylaminoethyl methacrylate)-*b*-poly(3-triisopropoxyethylpropyl methacrylate) ( $\mu$ -PDMS-*b*-PDMAEMA-*b*-PIPSMA).**  $\mu$ -PDMS-*b*-PDMAMEA-*b*-PIPSMA miktoarm star terpolymers were synthesized according to our previously reported procedure, as shown in Figure 2.<sup>40</sup> Azide-functionalized PDMS [PDMS-(OH,  $\text{N}_3$ )] (1) was synthesized according to the literature with a slight modification.<sup>52</sup> In a typical experiment, epoxide-terminated PDMS (15.5284 g, 3.1 mmol) was dissolved in isopropanol (75 mL), and then an aqueous solution of  $\text{NaN}_3$  (1.0093 g, 15.5 mmol) was added. The solution was adjusted to pH = 6.0 with glacial acetic acid. The reaction mixture was stirred at 50 °C until the  $^1\text{H}$  NMR signal of the starting material disappeared. After the reaction finished, hexane was added, followed by successively washing with saturated aqueous solution of  $\text{NaHCO}_3$ ,  $\text{H}_2\text{O}$ , and saturated NaCl solution. The organic layer was dried over anhydrous  $\text{MgSO}_4$  and then concentrated on a rotary evaporator and dried under vacuum overnight at room temperature.

The  $\alpha$ -alkynyl- $\omega$ -bromo-poly(*N,N*-dimethylaminoethyl methacrylate) (alkynyl-PDMAEMA-Br) was obtained by ATRP of DMAEMA, according to the literature with some modification.<sup>53</sup> The functional ATRP initiator propargyl 2-bromoisobutyrate (PBIB) was first prepared according to a method reported by Matyjaszewski.<sup>54</sup> Subsequently, in a typical procedure, PBIB (243.4 mg, 1.187 mmol), DMAEMA (20 mL, 118.7 mmol), HMTETA (273.5 mg, 1.187 mmol), and CuBr (170.3 mg, 1.187 mmol) were dissolved in a 20 mL anisole in a Schlenk tube. After three freeze–pump–thaw cycles, the Schlenk tube was sealed off, and the reaction mixture was allowed to proceed at 30 °C for 4.5 h. The reaction mixture was quickly cooled and diluted with THF. The copper salt was removed by passing through a neutral aluminum oxide column. After concentrating on a rotary evaporator, the mixture was precipitated into cold hexane. The product was purified by reprecipitation twice from THF to cold hexane and dried under vacuum overnight at 40 °C. (Yield: 64.7%).

The  $\alpha$ -alkynyl- $\omega$ -diethylamino-poly(*N,N*-dimethylaminoethyl methacrylate) (alkynyl-PDMAEMA- $\text{N}(\text{Et})_2$ ) (2) was obtained by dehalogenation of alkynyl-PDMAEMA-Br with excess of diethylamine. In a typical experiment, alkynyl-PDMAEMA-Br (11.90 g, 0.459 mmol), diethylamine (3.36 g, 45.9 mmol), and dimethylformamide (DMF) (100 mL) were sequentially added to a 250 mL round-bottomed flask and stirred at 80 °C for 36 h. DMF was removed by rotary evaporation, and the resulting crude product was dissolved in THF and precipitated in cold hexane. This step was repeated

three times and then dried under vacuum at 60 °C to give the brown product alkynyl-PDMAEMA-N(Et)<sub>2</sub> (8.20 g, 68.7%).

The poly(dimethylsiloxane)-(OH)-*b*-poly(*N,N*-dimethylaminoethyl methacrylate) (PDMS-(OH)-*b*-PDMAMEA) (3) diblock copolymer containing a hydroxyl group at the junction point was synthesized by the click reaction between 1 and 2. The diblock copolymer macroinitiators, namely PDMS-(Br)-*b*-PDMAEMA, were synthesized by the esterification reaction of PDMS-(OH)-*b*-PDMAMEA (3) with 2-bromoisobutryl bromide in pyridine. In a typical run, PDMS-(OH)-*b*-PDMAEMA (6.80 g, 0.220 mmol), DMAP (0.0671 g, 0.439 mmol), TEA (0.3558 g, 3.515 mmol), and anhydrous pyridine (200 mL) were sequentially added to a 250 mL three-necked round-bottomed flask, and stirred under a nitrogen atmosphere. Bromoisobutryl bromide (0.7578 g, 3.296 mmol) was added dropwise at 0 °C, followed by stirring for 48 h. The pyridine was removed by rotary evaporation, and the residue was dissolved with THF and then precipitated in cold hexane. The yellow product was purified by reprecipitating twice from THF to cold hexane and dried under vacuum at 40 °C overnight. (3.90 g, 56.9%).

$\mu$ -PDMS-*b*-PDMAMEA-*b*-PIPSMA ABC miktoarm terpolymers were synthesized by ATRP polymerization of IPSMA using PDMS-(Br)-*b*-PDMAEMA as the initiator. In a typical run, PDMS-(Br)-*b*-PDMAEMA (1.00 g, 0.032 mmol), IPSMA (0.3464 g, 0.962 mmol), isopropyl alcohol (3.0 mL), PMDETA (6.1 mg, 0.032 mmol), and CuBr (5.1 mg, 0.032 mmol) were sequentially added into a Schlenk tube. After three freeze–pump–thaw cycles, the Schlenk tube was sealed off, and the reaction mixture was allowed to proceed at 50 °C for about 12 h. The reaction mixture was quickly cooled and diluted with THF. The copper salt was removed by passing through a neutral aluminum oxide column. After concentrating on a rotary evaporator, the mixture was precipitated into cold hexane. The product was purified by reprecipitating twice from THF to cold hexane and dried under vacuum at room temperature overnight. (Yield: 64.6%).

**Cotton Coating.** The coating procedure was carried out according to the literature.<sup>31</sup> To coat fabric samples, swatches at 3 × 3 cm<sup>2</sup> were dipped into the respective polymer solutions (30 mg/mL) for 30 min. The swatches were withdrawn from the solution and heated at 180 °C for 4 h under vacuum. Subsequently, fabrics were extracted with a Soxhlet extractor in THF for 8 h. After extraction, the fabric samples were dried under vacuum for 24 h. The mass fraction of grafted block copolymers was determined by gravimetric analysis and thermogravimetric analysis.

**Separation of Heavy Oil–Water–Light Oil Ternary Mixtures.** The membrane was prewetted by hexane before being fixed between two frosted glass fixtures. Dichloroethane–water–hexane ternary mixtures were investigated in this work. These oils were tinted with oil red. A 45 mL volume of the heavy oil–water–light oil ternary mixtures (volume ratio = 1:1:1) was added to an upper glass tube before contacting with the prewetted membrane. The separation process was driven only by gravity.

**Characterization.** Size exclusion chromatography (SEC) was used to measure the polydispersity index (PDI) of all the polymers. The SEC was equipped with a Waters 2414 refractive index detector and a Waters 515 high-performance liquid chromatography pump. THF was used as the eluent, and the flow rate is 1.0 mL/min. The molecular weight and PDI were calculated using monodispersed polystyrene as the

calibration standard. The <sup>1</sup>H NMR spectra were recorded on a Bruker AVANCE III 600 NMR spectrometer. SEM observations were performed using Zeiss EVO 18 operating at 10 kV. XPS spectra were obtained on a Thermo Fisher Scientific spectrometer (ESCALAB 250Xi) with a micro-focused raster-scanned X-ray beam. The take-off angle is 90°. FTIR spectra were recorded on a Bruker Vector 70 FTIR spectrometer. CAs of water or oil droplets (5.0  $\mu$ L) were measured on a Data Physics OCA 20 instrument. At least five different points on the samples were measured.

## ■ ASSOCIATED CONTENT

### 📄 Supporting Information

The Supporting Information is available free of charge on the ACS Publications website at DOI: 10.1021/acsomega.9b01235.

DCE-water separation (MP4)

Water-hexane separation (MP4)

Ternary oil–water separation (MP4)

NMR spectra; SEM image of cotton fabric used; TGA of pristine cotton fabrics and functionalized cotton fabrics; mass fraction of grafted block copolymers; XPS spectra of pristine cotton fabrics and functionalized cotton fabrics; and relationship between breakthrough pressure and CA (PDF)

## ■ AUTHOR INFORMATION

### Corresponding Author

\*E-mail: mslzhong@scut.edu.cn.

### ORCID

Liangzhi Hong: 0000-0002-2297-8013

### Notes

The authors declare no competing financial interest.

## ■ ACKNOWLEDGMENTS

This work is supported by the National Natural Science Foundation of China (grant nos. 21774035, 21374031).

## ■ REFERENCES

- (1) Gupta, R. K.; Dunderdale, G. J.; England, M. W.; Hozumi, A. Oil/water separation techniques: a review of recent progresses and future directions. *J. Mater. Chem. A* **2017**, *5*, 16025–16058.
- (2) Ge, M.; Cao, C.; Huang, J.; Zhang, X.; Tang, Y.; Zhou, X.; Zhang, K.; Chen, Z.; Lai, Y. Rational design of materials interface at nanoscale towards intelligent oil-water separation. *Nanoscale Horiz.* **2018**, *3*, 235–260.
- (3) Xue, Z.; Cao, Y.; Liu, N.; Feng, L.; Jiang, L. Special wettable materials for oil/water separation. *J. Mater. Chem. A* **2014**, *2*, 2445–2460.
- (4) Chu, Z.; Feng, Y.; Seeger, S. Oil/Water Separation with Selective Superantwetting/Superwetting Surface Materials. *Angew. Chem., Int. Ed.* **2015**, *54*, 2328–2338.
- (5) Kwon, G.; Post, E.; Tuteja, A. Membranes with selective wettability for the separation of oil-water mixtures. *MRS Commun.* **2015**, *5*, 475–494.
- (6) Feng, L.; Zhang, Z.; Mai, Z.; Ma, Y.; Liu, B.; Jiang, L.; Zhu, D. A super-hydrophobic and super-oleophilic coating mesh film for the separation of oil and water. *Angew. Chem., Int. Ed.* **2004**, *43*, 2012–2014.
- (7) Liu, M.; Wang, S.; Wei, Z.; Song, Y.; Jiang, L. Bioinspired Design of a Superoleophobic and Low Adhesive Water/Solid Interface. *Adv. Mater.* **2009**, *21*, 665–669.

- (8) Ma, Q.; Cheng, H.; Fane, A. G.; Wang, R.; Zhang, H. Recent Development of Advanced Materials with Special Wettability for Selective Oil/Water Separation. *Small* **2016**, *12*, 2186–2202.
- (9) Wang, B.; Liang, W.; Guo, Z.; Liu, W. Biomimetic superlyophobic and superlyophilic materials applied for oil/water separation: a new strategy beyond nature. *Chem. Soc. Rev.* **2015**, *44*, 336–361.
- (10) Wei, Y.; Qi, H.; Gong, X.; Zhao, S. Specially Wettable Membranes for Oil-Water Separation. *Adv. Mater. Interfaces* **2018**, *5*, 1800576.
- (11) Ren, G.; Song, Y.; Li, X.; Zhou, Y.; Zhang, Z.; Zhu, X. A Superhydrophobic Copper Mesh as an Advanced Platform for Oil-Water Separation. *Appl. Surf. Sci.* **2018**, *428*, 520–525.
- (12) Zhu, X.; Zhang, Z.; Song, Y.; Yan, J.; Wang, Y.; Ren, G. A Waterproofing Textile with Robust Superhydrophobicity in either Air or Oil Surroundings. *J. Taiwan Inst. Chem. Eng.* **2017**, *71*, 421–425.
- (13) Shi, B.; Jia, X.; Guo, Z. An easy preparation of photo-response TiO<sub>2</sub>@copper wire mesh with quick on/off switchable superwetting for high efficiency oil-water separation. *New J. Chem.* **2018**, *42*, 17563–17573.
- (14) Ge, D.; Yang, L.; Wang, C.; Lee, E.; Zhang, Y.; Yang, S. A multi-functional oil-water separator from a selectively pre-wetted superamphiphobic paper. *Chem. Commun.* **2015**, *51*, 6149–6152.
- (15) Li, J.-J.; Zhou, Y.-N.; Luo, Z.-H. Smart Fiber Membrane for pH-Induced Oil/Water Separation. *ACS Appl. Mater. Interfaces* **2015**, *7*, 19643–19650.
- (16) Zhou, Y.-N.; Li, J.-J.; Luo, Z.-H. Toward Efficient Water/Oil Separation Material: Effect of Copolymer Composition on pH-Responsive Wettability and Separation Performance. *AIChE J.* **2016**, *62*, 1758–1771.
- (17) Zhang, L.; Zhang, Z.; Wang, P. Smart surfaces with switchable superoleophilicity and superoleophobicity in aqueous media: toward controllable oil/water separation. *NPG Asia Mater.* **2012**, *4*, No. e8.
- (18) Wang, B.; Guo, Z. pH-responsive bidirectional oil-water separation material. *Chem. Commun.* **2013**, *49*, 9416–9418.
- (19) Ju, G.; Cheng, M.; Shi, F. A pH-responsive smart surface for the continuous separation of oil/water/oil ternary mixtures. *NPG Asia Mater.* **2014**, *6*, No. e111.
- (20) Cheng, Z.; Wang, J.; Lai, H.; Du, Y.; Hou, R.; Li, C.; Zhang, N.; Sun, K. pH-Controllable On-Demand Oil/Water Separation on the Switchable Superhydrophobic/Superhydrophilic and Underwater Low-Adhesive Superoleophobic Copper Mesh Film. *Langmuir* **2015**, *31*, 1393–1399.
- (21) Xu, Z.; Zhao, Y.; Wang, H.; Zhou, H.; Qin, C.; Wang, X.; Lin, T. Fluorine-Free Superhydrophobic Coatings with pH-induced Wettability Transition for Controllable Oil-Water Separation. *ACS Appl. Mater. Interfaces* **2016**, *8*, 5661–5667.
- (22) Ou, R.; Wei, J.; Jiang, L.; Simon, G. P.; Wang, H. Robust Thermoresponsive Polymer Composite Membrane with Switchable Superhydrophilicity and Superhydrophobicity for Efficient Oil-Water Separation. *Environ. Sci. Technol.* **2016**, *50*, 906–914.
- (23) Li, J.-J.; Zhu, L.-T.; Luo, Z.-H. Electrospun fibrous membrane with enhanced switchable oil/water wettability for oily water separation. *Chem. Eng. J.* **2016**, *287*, 474–481.
- (24) Xue, B.; Gao, L.; Hou, Y.; Liu, Z.; Jiang, L. Temperature Controlled Water/Oil Wettability of a Surface Fabricated by a Block Copolymer: Application as a Dual Water/Oil On-Off Switch. *Adv. Mater.* **2013**, *25*, 273–277.
- (25) Cao, Y.; Liu, N.; Fu, C.; Li, K.; Tao, L.; Feng, L.; Wei, Y. Thermo and pH Dual-Responsive Materials for Controllable Oil/Water Separation. *ACS Appl. Mater. Interfaces* **2014**, *6*, 2026–2030.
- (26) Tian, D.; Zhang, X.; Tian, Y.; Wu, Y.; Wang, X.; Zhai, J.; Jiang, L. Photo-induced water-oil separation based on switchable superhydrophobicity-superhydrophilicity and underwater superoleophobicity of the aligned ZnO nanorod array-coated mesh films. *J. Mater. Chem.* **2012**, *22*, 19652–19657.
- (27) Zheng, X.; Guo, Z.; Tian, D.; Zhang, X.; Jiang, L. Electric Field Induced Switchable Wettability to Water on the Polyaniline Membrane and Oil/Water Separation. *Adv. Mater. Interfaces* **2016**, *3*, 1600461.
- (28) Kwon, G.; Kota, A. K.; Li, Y.; Sohani, A.; Mabry, J. M.; Tuteja, A. On-Demand Separation of Oil-Water Mixtures. *Adv. Mater.* **2012**, *24*, 3666–3671.
- (29) Che, H.; Huo, M.; Peng, L.; Fang, T.; Liu, N.; Feng, L.; Wei, Y.; Yuan, J. CO<sub>2</sub>-Responsive Nanofibrous Membranes with Switchable Oil/Water Wettability. *Angew. Chem., Int. Ed.* **2015**, *54*, 8934–8938.
- (30) Liu, N.; Cao, Y.; Lin, X.; Chen, Y.; Feng, L.; Wei, Y. A Facile Solvent-Manipulated Mesh for Reversible Oil/Water Separation. *ACS Appl. Mater. Interfaces* **2014**, *6*, 12821–12826.
- (31) Li, J.-J.; Zhou, Y.-N.; Luo, Z.-H. Polymeric Materials with Switchable Superwettability for Controllable Oil/Water Separation: A Comprehensive Review. *Prog. Polym. Sci.* **2018**, *87*, 1–33.
- (32) Kota, A. K.; Kwon, G.; Choi, W.; Mabry, J. M.; Tuteja, A. Hygro-responsive membranes for effective oil-water separation. *Nat. Commun.* **2012**, *3*, 1025.
- (33) Wang, Z.; Wang, Y.; Liu, G. Rapid and Efficient Separation of Oil from Oil-in-Water Emulsions Using a Janus Cotton Fabric. *Angew. Chem., Int. Ed.* **2016**, *55*, 1291–1294.
- (34) Wang, Z.; Lehtinen, M.; Liu, G. Universal Janus Filters for the Rapid Separation of Oil from Emulsions Stabilized by Ionic or Nonionic Surfactants. *Angew. Chem., Int. Ed.* **2017**, *56*, 12892–12897.
- (35) Wang, Z.; Liu, G.; Huang, S. In Situ Generated Janus Fabrics for the Rapid and Efficient Separation of Oil from Oil-in-Water Emulsions. *Angew. Chem., Int. Ed.* **2016**, *55*, 14610–14613.
- (36) Cao, G.; Zhang, W.; Jia, Z.; Liu, F.; Yang, H.; Yu, Q.; Wang, Y.; Di, X.; Wang, C.; Ho, S.-H. Dually Prewetted Underwater Superoleophobic and under Oil Superhydrophobic Fabric for Successive Separation of Light Oil/Water/Heavy Oil Three-Phase Mixtures. *ACS Appl. Mater. Interfaces* **2017**, *9*, 36368–36376.
- (37) Cao, G.; Wang, Y.; Wang, C.; Ho, S.-H. A Dually Prewetted Membrane for Continuous Filtration of Water-in-Light Oil, Oil-in-Water, and Water-in-Heavy Oil Multiphase Emulsion Mixtures. *J. Mater. Chem. A* **2019**, *7*, 11305–11313.
- (38) Bosq, N.; Guigo, N.; Persello, J.; Sbirrazzuoli, N. Melt and glass crystallization of PDMS and PDMS silica nanocomposites. *Phys. Chem. Chem. Phys.* **2014**, *16*, 7830–7840.
- (39) Hunley, M. T.; England, J. P.; Long, T. E. Influence of Counteranion on the Thermal and Solution Behavior of Poly(2-(dimethylamino)ethyl methacrylate)-Based Polyelectrolytes. *Macromolecules* **2010**, *43*, 9998–10005.
- (40) Liu, M.; Chen, X.; Yang, Z.; Xu, Z.; Hong, L.; Ngai, T. Tunable Pickering Emulsions with Environmentally Responsive Hairy Silica Nanoparticles. *ACS Appl. Mater. Interfaces* **2016**, *8*, 32250–32258.
- (41) Gao, H.; Zhao, Z.; Cai, Y.; Zhou, J.; Hua, W.; Chen, L.; Wang, L.; Zhang, J.; Han, D.; Liu, M.; Jiang, L. Adaptive and freeze-tolerant heteronetwork organohydrogels with enhanced mechanical stability over a wide temperature range. *Nat. Commun.* **2017**, *8*, 15911.
- (42) Li, C.; Ge, Z.; Fang, J.; Liu, S. Synthesis and Self-Assembly of Coil-Rod Double Hydrophilic Diblock Copolymer with Dually Responsive Asymmetric Centipede-Shaped Polymer Brush as the Rod Segment. *Macromolecules* **2009**, *42*, 2916–2924.
- (43) Sun, W.; He, X.; Gao, C.; Liao, X.; Xie, M.; Lin, S.; Yan, D. Novel Amphiphilic and Photo-Responsive ABC 3-miktoarm Star Terpolymers: Synthesis, Self-Assembly and Photo-Responsive Behavior. *Polym. Chem.* **2013**, *4*, 1939–1949.
- (44) Li, J.-J.; Zhou, Y.-N.; Luo, Z.-H. Mussel-inspired V-shaped copolymer coating for intelligent oil/water separation. *Chem. Eng. J.* **2017**, *322*, 693–701.
- (45) Roy, D.; Knapp, J. S.; Guthrie, J. T.; Perrier, S. Antibacterial cellulose fiber via RAFT surface graft polymerization. *Biomacromolecules* **2008**, *9*, 91–99.
- (46) van de Wetering, P.; Zuidam, N. J.; van Steenberg, M. J.; van der Houwen, O. A. G. J.; Underberg, W. J. M.; Hennink, W. E. A mechanistic study of the hydrolytic stability of poly(2-(dimethylamino)ethyl methacrylate). *Macromolecules* **1998**, *31*, 8063–8068.



- (47) Tian, X.; Jokinen, V.; Li, J.; Sainio, J.; Ras, R. H. A. Unusual Dual Superlyophobic Surfaces in Oil-Water Systems: The Design Principles. *Adv. Mater.* **2016**, *28*, 10652.
- (48) Hou, X.; Hu, Y.; Grinthal, A.; Khan, M.; Aizenberg, J. Liquid-based gating mechanism with tunable multiphase selectivity and antifouling behaviour. *Nature* **2015**, *519*, 70–73.
- (49) Choi, W.; Tuteja, A.; Chhatre, S.; Mabry, J. M.; Cohen, R. E.; McKinley, G. H. Fabrics with Tunable Oleophobicity. *Adv. Mater.* **2009**, *21*, 2190–2195.
- (50) Zhang, W.; Liu, N.; Zhang, Q.; Qu, R.; Liu, Y.; Li, X.; Wei, Y.; Feng, L.; Jiang, L. Thermo-Driven Controllable Emulsion Separation by a Polymer-Decorated Membrane with Switchable Wettability. *Angew. Chem., Int. Ed.* **2018**, *57*, 5740–5745.
- (51) Ozaki, H.; Hirao, A.; Nakahama, S. Polymerization of Monomers Containing Functional Silyl Groups. 11. Anionic Living Polymerization of 3-(Tri-2-propoxysilyl)propyl Methacrylate. *Macromolecules* **1992**, *25*, 1391–1395.
- (52) Halila, S.; Manguian, M.; Fort, S.; Cottaz, S.; Hamaide, T.; Fleury, E.; Driguez, H. Syntheses of Well-Defined Glyco-Polyorganosiloxanes by "Click" Chemistry and their Surfactant Properties. *Macromol. Chem. Phys.* **2008**, *209*, 1282–1290.
- (53) Zhang, X.; Xia, J.; Matyjaszewski, K. Controlled/"Living" Radical Polymerization of 2-(Dimethylamino)ethyl Methacrylate. *Macromolecules* **1998**, *31*, 5167–5169.
- (54) Tsarevsky, N. V.; Sumerlin, B. S.; Matyjaszewski, K. Step-Growth "Click" Coupling of Telechelic Polymers Prepared by Atom Transfer Radical Polymerization. *Macromolecules* **2005**, *38*, 3558–3561.